Princeton Plasma Physics Laboratory

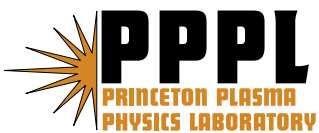## MHD Induced Neutral Beam Ion Loss
from NSTX Plasmas

D.S. Darrow, E.D. Fredrickson, N.N. Gorelenkov,
A.L. Roquemore, and K. Shinohara

November 2007

Princeton Plasma Physics Laboratory
Report Disclaimers

Full Legal Disclaimer

This report was prepared as an account of work sponsored by an agency of the United States Government. Neither the United States Government nor any agency thereof, nor any of their employees, nor any of their contractors, subcontractors or their employees, makes any warranty, express or implied, or assumes any legal liability or responsibility for the accuracy, completeness, or any third party's use or the results of such use of any information, apparatus, product, or process disclosed, or represents that its use would not infringe privately owned rights. Reference herein to any specific commercial product, process, or service by trade name, trademark, manufacturer, or otherwise, does not necessarily constitute or imply its endorsement, recommendation, or favoring by the United States Government or any agency thereof or its contractors or subcontractors. The views and opinions of authors expressed herein do not necessarily state or reflect those of the United States Government or any agency thereof.

Trademark Disclaimer

Reference herein to any specific commercial product, process, or service by trade name, trademark, manufacturer, or otherwise, does not necessarily constitute or imply its endorsement, recommendation, or favoring by the United States Government or any agency thereof or its contractors or subcontractors.

PPPL Report Availability

Princeton Plasma Physics Laboratory:

http://www.pppl.gov/techreports.cfm

Office of Scientific and Technical Information (OSTI):

http://www.osti.gov/bridge

Related Links:

U.S. Department of Energy

Office of Scientific and Technical Information

Fusion Links

MHD Induced Neutral Beam Ion Loss from NSTX Plasmas

D S Darrow[1], E D Fredrickson[1], N N Gorelenkov[1], A L Roquemore[1], K Shinohara[2]

[1]Princeton Plasma Physics Laboratory, PO Box 451, Princeton, NJ 08543-0451, USA

[2]Japan Atomic Energy Agency, Naka, Ibaraki, Japan

Abstract

Bursts of ~60 kHz activity on Mirnov coils occur frequently in NSTX plasmas and these are accompanied by bursts of neutral beam ion loss over a range in pitch angles. These losses have been measured with a scintillator type loss probe imaged with a high speed (>10,000 frames/s) video camera, giving the evolution of the energy and pitch angle distributions of the lost neutral beam ions over the course of the events. The instability occurs below the TAE frequency in NSTX (~100 kHz) in high beta plasmas and may be a beta driven Alfvén acoustic (BAAE) mode.
The data from one burst that causes a 13% reduction in the neutron rate has been studied extensively and has several interesting features. First, the burst begins with the mode having a purely n=1 character, sweeping downward in frequency. However, there is no change to the underlying loss signal during this time interval. This indicates there is no phase space transport of fast (80 keV D) ions into the loss cone seen by the probe from the frequency sweeping. As the burst evolves further in time, a concurrent n=2 mode arises, followed quickly by a concurrent n=3 mode. During this period when multiple modes are present, loss over a wide range of pitch angles is seen simultaneously, suggesting stochastization of the beam ion phase space. There is no evidence of any sweeping in pitch angle of the loss in either phase of the burst, at least not on the 100 microsecond time scale.

1. Introduction

Magnetohydrodynamic (MHD) instabilities in magnetically confined plasmas can often be driven by a population of superthermal ions. In addition, such, instabilities can often cause the loss of energetic ions from the plasma. The National Spherical Torus Experiment NSTX)[1] is a low aspect ratio tokamak heated by up to 8 MW of 90 kV deuterium neutral beams. Here, we describe observations of a bursting MHD mode driven by energetic neutral beam heating ions and which is detected by a Mirnov coil outside the plasma and which produces loss of those fast ions to a detector located at the vacuum vessel wall. The fast ion loss detector in NSTX[2] is of a scintillator type, which measures the pitch angle and gyroradius of the lost ions as a function of time. The probe acts as a magnetic spectrometer, using a pair of apertures and the confining magnetic field of the plasma to disperse lost fast ions onto a scintillator plate where their strike point is determined by their pitch angle and gyroradius. For this experiment, the luminosity pattern on the scintillator plate was imaged by a fast framing rate intensified video camera

(Photron Fastcam operated at 13,500 frames/s) in order to obtain high time resolution of the parameters of the lost ions.

2. Results

Figure 1 displays the time evolution of the plasma current, neutral beam heating power, and neutron rate of NSTX pulse 119624. In the portion of the pulse between the solid vertical lines in this figure, numerous rapid drops in the neutron rate are observed. These drops in the neutron rate coincide with brief bursts of MHD activity detected by a Mirnov coil in the vacuum vessel. The frequency spectrogram of these bursts is shown in figure 2. Such bursts occur commonly and repeatedly in NSTX discharges over a wide range in parameters. We choose to focus on the burst at 194 ms as a typical case. Figure 3 shows the evolution of the neutron rate before, during, and after this burst, which results in ~13% drop in the neutron rate, indicative of the loss of a significant fraction of the neutral beam ions in the plasma, as neutron production in NSTX is essentially all due to beam-plasma reactions and the plasma density profile does not change appreciably during these events. Note that the drop in neutron rate commences at about 194.3 ms.

Figure 4 shows the frequency spectrogram of the burst on an expanded time scale. The burst can be divided into two intervals in time. It starts as an n=1 mode at 65 kHz, which chirps downward in frequency to 40 kHz in the course of 0.5 ms. Toward the end of the frequency chirp, an n=2 mode arises and, shortly thereafter, an n=3 mode also develops. In this phase of the burst, at least two modes of different n numbers are present concurrently until the burst ends. Figure 5 shows the spectrum of the Alfvén continuum for this time in the discharge, as calculated by the ideal MHD code NOVA-K[5]. The n=3 mode seen in figure 4 lies in the middle of the beta induced Alfvén acoustic eigenmode (BAAE)[4] gap marked in the figure. This mode appears at 18 kHz in the plasma rest frame. At this time in the discharge, the plasma is rotating with a frequency of 20 kHz, giving a predicted mode frequency in the lab frame of 78 kHz. This is identical to the observed frequency shown in figure 4, meaning that this mode is quite possibly a BAAE. Shown also in figure 3 are two modes close in frequency, namely a 17kHz BAAE localized closer to the core and a 35kHz beta-induced Alfvén eigenmode (BAE)[6], which are also candidate identifications of this mode, given the uncertainties in the rotation velocity and the mode location measurements.

Figure 6 shows images from the fast ion loss probe during the initial phase of the burst. In this and the succeeding figure, the starting times of each frame, as reported by the camera's internal clock, are shown. These times are found to be synchronized with the NSTX digitizer times to within half a camera frame duration (36 μs). Before and during the frequency chirping portion of the burst, the loss images look identical to image A. This image shows a single luminous spot consistent with loss at a single pitch angle and gyroradius. This spot first appears when neutral beam source C (which is the most perpendicular of the three beam sources on NSTX and which has a tangency radius of 50 cm) starts injecting and it is interpreted as prompt orbit loss from that beam. This spot is steady in position, size, and luminosity before the burst begins and through the frequency chirping phase of the burst as well. Indeed, it appears that this spot is constant before, during, and after the burst, which would be consistent with prompt loss behavior during steady beam injection. In the later phases of the burst, there is loss evident at other positions on the scintillator, but those losses appear additive to this underlying prompt loss. Images B and C in figure 6 show the loss probe images as the burst enters the mode overlap or multi-n phase. Here, there total luminosity is greater. Note that the onset of the broad range of pitch angle loss in frame B of figure 6, taken at 194.296 ms, coincides with the time at which the total neutron rate begins its precipitous drop. The position of the luminosity in the scintillator plate in the images in

figure 6 is consistent with loss of D beam ions at the primary injection energy of 90 kV, but lost over a wide range in pitch angles, in contrast to the single pitch angle of loss in frame A. (See figure 8 for the interpretation grid of pitch angle and gyroradius.) This transient loss of a wide range of pitch angles is similar to beam ion loss features seen in Alfvénic modes in the CHS device[3].

Figure 7 displays the loss probe images in the later part of the burst as the concurrent modes decay. During this interval, the beam C prompt loss persists, but the wide pitch angle loss dims and then vanishes. The wide pitch angle loss vanishes as the mode overlap ends, suggesting strongly that it is this overlap which is responsible for the wide range of pitch angles lost. Frame E, taken starting at 194.519 ms, evidences the last significant traces of the broad range of lost pitch angles, and the total luminosity in this frame is clearly less than in frames B, C, or D. This time correlates well with the time in figure 3 at which the neutron rate ceases to fall and reverts to its pre-burst rate of increase.

Figure 8 shows loss image B, taken when the multiple n number modes begin to overlap, with a superimposed grid to allow determination of the pitch angle and gyroradius of the lost ions. The image is consistent with D beam ion loss at the full injection energy of 90 kV, and covering a range in pitch angle from 15° to 63°, i.e. from fairly parallel going to fairly perpendicular moving.

3. Interpretation

The scintillator loss probe images do not show any significant change in the beam ion loss rate or characteristics before or during the frequency chirping phase of this burst. From theoretical considerations, one might expect that a frequency chirping mode could alter the energy or canonical angular momentum of fast ions, or both. A change in canonical angular momentum could result in radial transport of the affected particle. Certainly, no change in energy of the lost ions is seen during the chirping phase of the burst. Given that no change in the loss characteristics is seen during the chirping phase, we conclude that either the frequency chirp is not causing radial transport of the fast ions, or is at least not causing transport into the loss cone at a point where the fast ion loss probe can detect it. Secondly, we note that losses which are driven by the burst arise only at times when there are concurrent multiple n number modes present, e.g. during frames B, C, D, and E in figures 6 & 7. These losses are at the primary beam injection energy and cover a wide range in pitch angle, as seen in figure 8. This loss during mode overlap is also seen to turn on and off quite quickly as the multiple n mode overlap starts and ends. The start and end times of the broad pitch angle loss coincide with the interval over which the neutron rate is dropping. Furthermore, the fast ion loss during the concurrent multiple n mode phase of the burst does not show any evidence of sweeping or moving in pitch angle, at least not on a time scale that could be imaged by the camera used (73 μs/frame). This sweeping in pitch angle is something that might be expected to occur if resonance between modes and particles were causing the wide range of lost pitch angles seen. From these features, we believe that the wide pitch angle range lost arises from a stochastization of the fast ion phase space induced by the presence of multiple n-number modes (i.e. modes of differing helicities or spatial structures.) We do note, however, that locally stronger features of the loss, such as the two brighter spots toward the lower left of image B in figure 6 may arise from resonant mode-particle interactions.

(Encouragement of Young Scientists (B) No 16760681).

References

[1]J. Spitzer, M. Ono, M. Peng, *et al., Fusion Technology* **30**, 1337 (1996).
[2]D. S. Darrow, accepted for publication in *Rev. Sci. Instrum,* (2007).
[3]K. Shinohara, M. Isobe, D. S. Darrow, A. Shimizu, K. Nagaoka, and S. Okamura, Plasma and Fusion Research, **2**, 042 (2007).
[4]N. N. Gorelenkov, H. L. Berk, E. Fredrickson, S. E. Sharapov, *Phys. Letters A, .***370/1**, 70 (2007).
[5]C. Z. Cheng, M. S. Chance, *Phys. Fluids*, **29**, 3695 (1986).
[6]A. D. Turnbull, E. J. Strait, W. W. Heidbrink, *et.al., Phys. Fluids B* **5**, 2546 (1995).

Figures
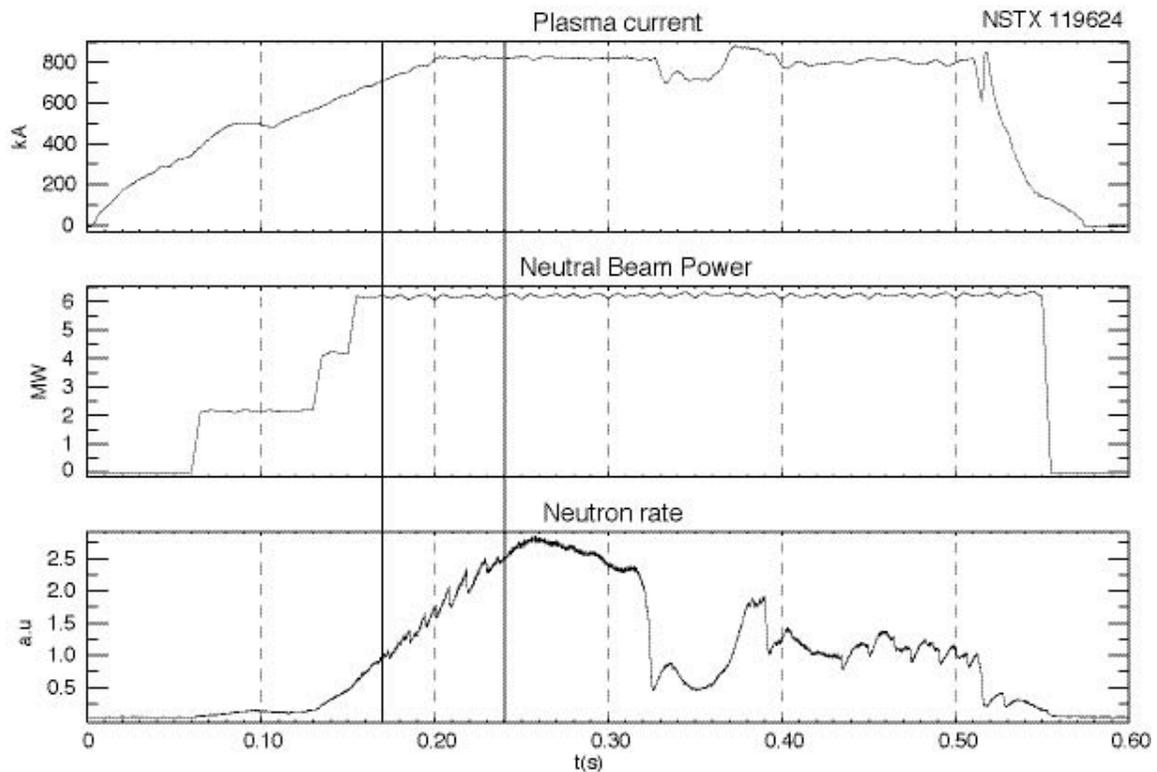
Figure 1: Plasma current in (kA) in the top panel, neutral beam power (MW) in the middle panel, and neutron rate (a. u.) in the bottom panel for NSTX pulse number 119624. During the interval outlined by the two solid vertical lines, there are repeated drops in the neutron rate that are attributable to Energetic Particle Modes (EPMs).
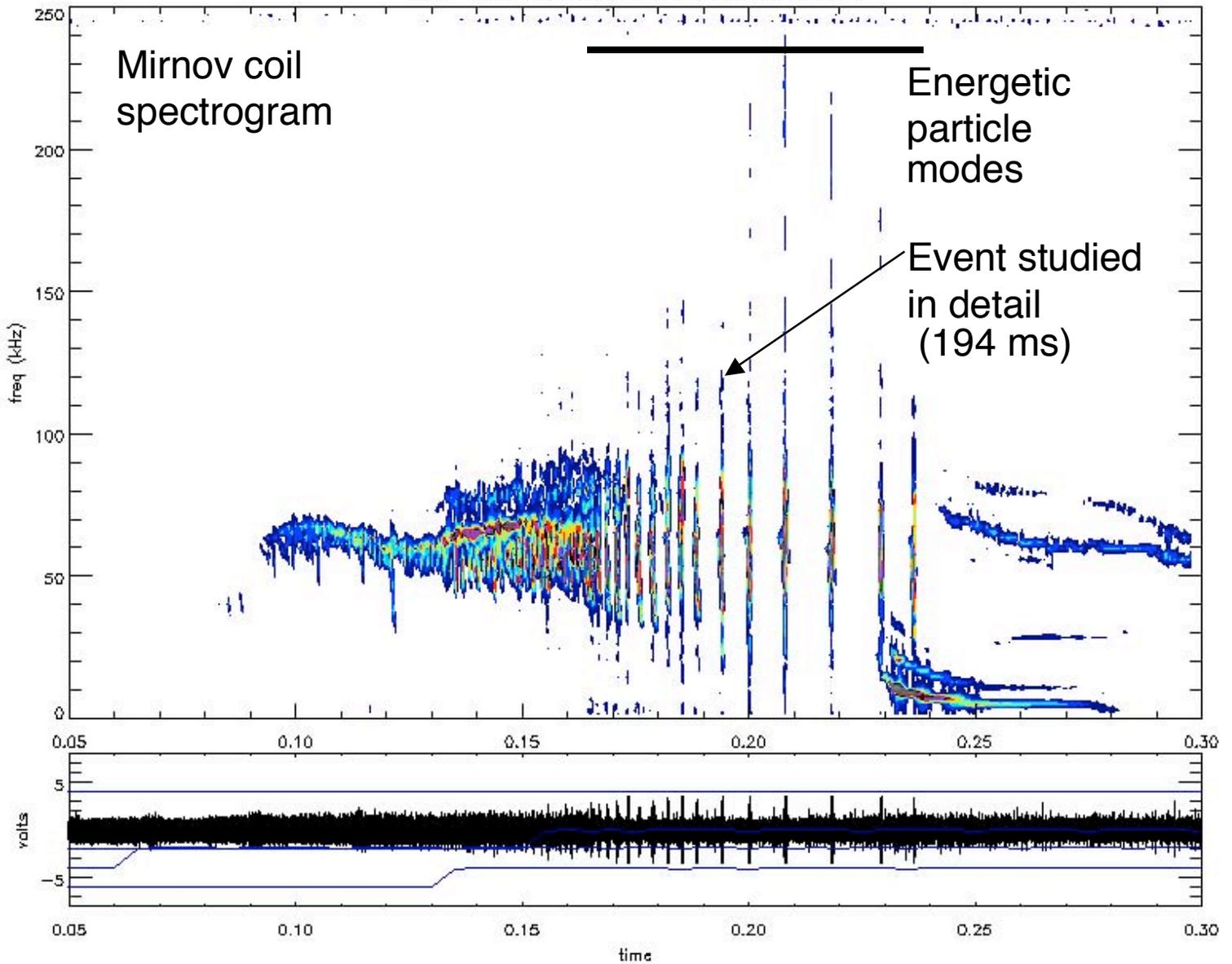
Figure 2: The upper panel shows the frequency spectrogram of magnetic fluctuations vs time in pulse 119624. Note the repeated short EPM bursts occurring during the interval marked by the bar near the top of the plot. The lower panel shows the raw Mirnov coil voltage vs time. In this paper, detailed analysis is made of the event marked by the arrow, at 194 ms.
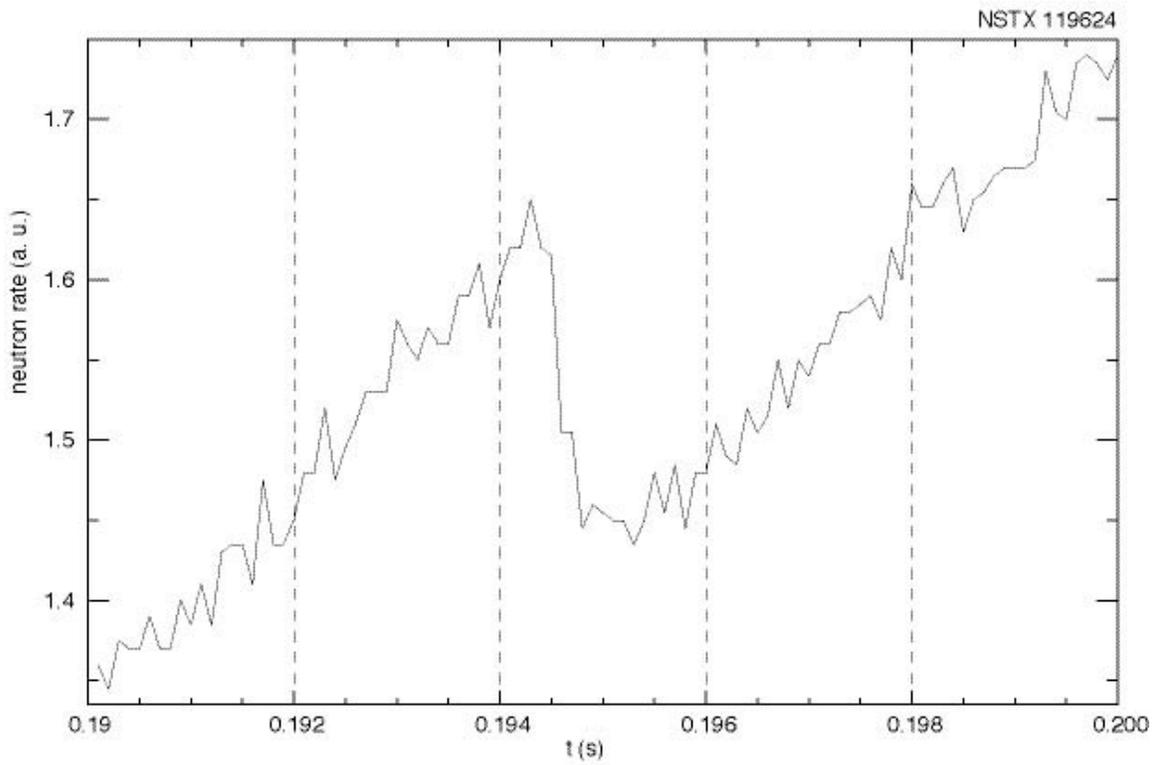
Figure 3: Neutron rate versus time over the course of the burst under study. The total neutron rate drops by 13 percent as a result of the single burst, with the drop in rate beginning at ~194.3 ms.
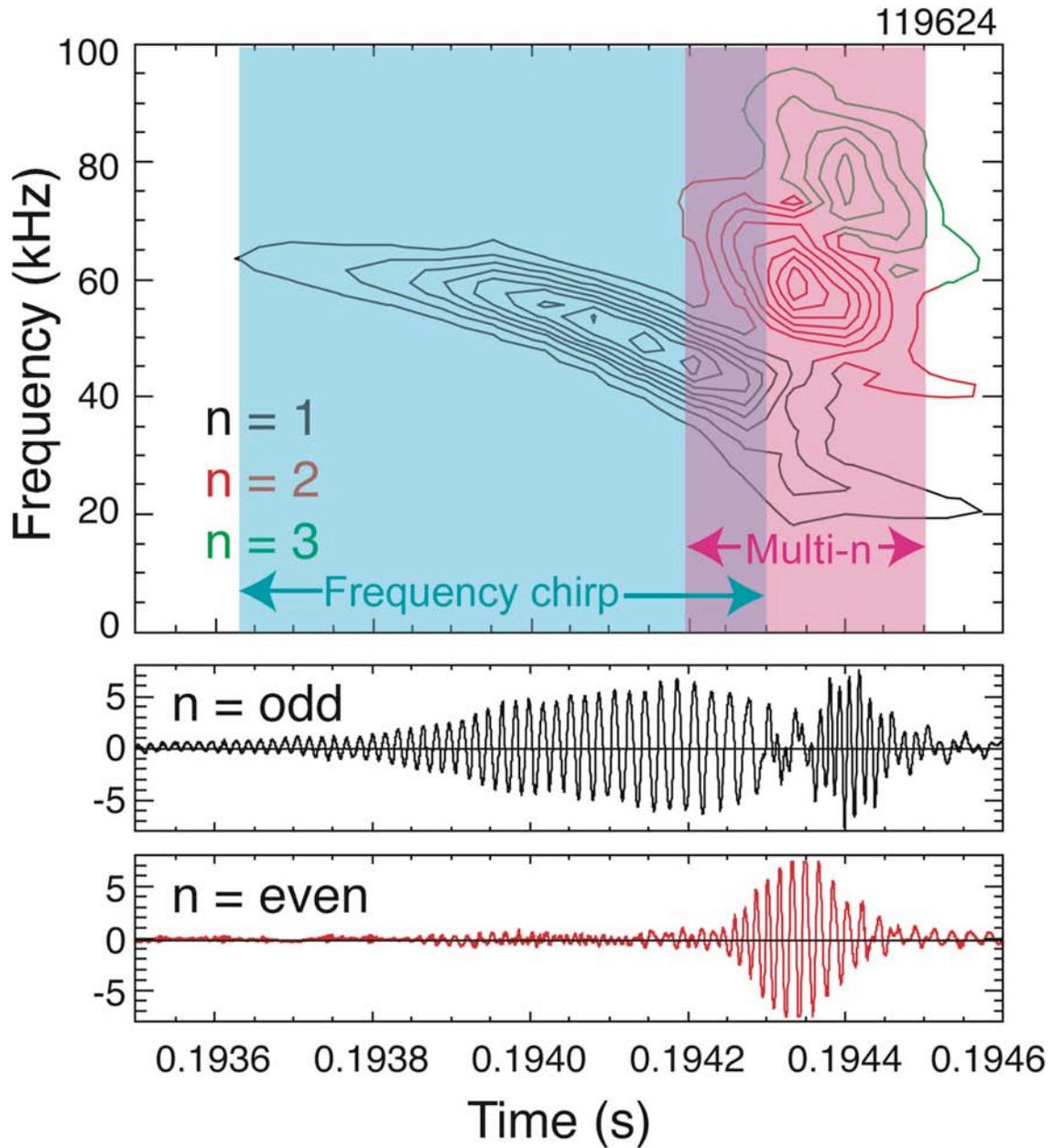
Figure 4: Expanded frequency spectrogram of the burst under study. The upper panel shows contours of mode amplitude versus frequency and time. The burst commences as a mode with a toroidal mode number n=1 which chirps downward in frequency. This is shown in the black amplitude contours, and the period of frequency chirping is outlined in pale blue. Subsequently, the mode spawns an n=2 mode, shown in the red contours, that exists concurrently with the n=1 mode. Shortly thereafter, an n=3 mode also arises, shown in the green contours. During this interval, outlined by the lavender box and labeled "multi-n," at least two different n number modes exist concurrently. The middle panel shows the Mirnov coil signal, filtered to retain only the signal coming from the odd n number modes. The bottom panel shows the Mirnov coil signal, but filtered to retain only the signal attributable to even n number modes.
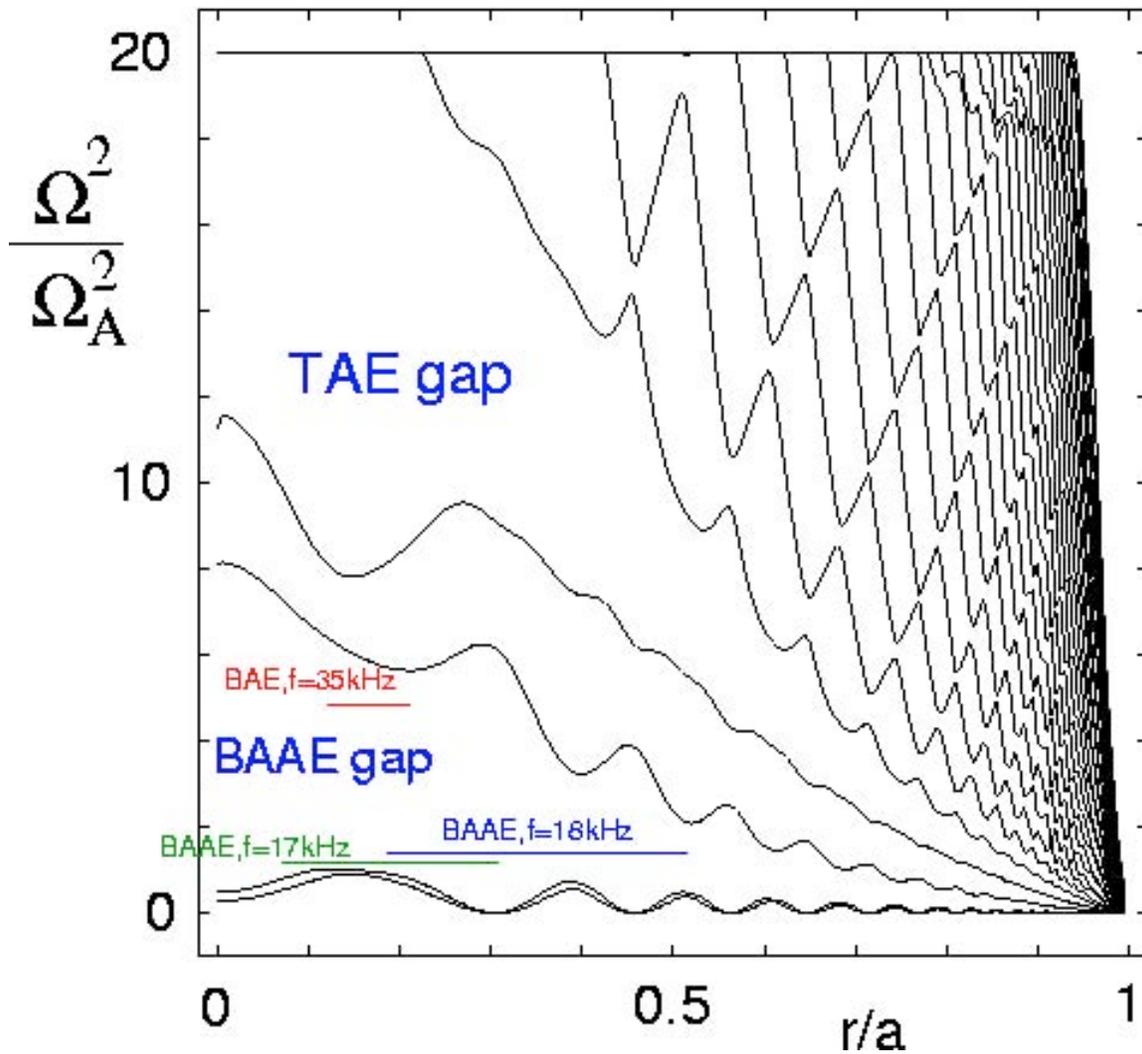
Figure 5: The Alfvén and acoustic gap diagram for this plasma at the time of the burst. This calculation shows a clear beta-induced Alfvén acoustic eigenmode (BAAE) gap for n=3 at 18 kHz. The plasma rotation frequency at this time in the discharge is 20 kHz, giving a predicted mode frequency in the lab frame of 78 kHz for the n=3 mode. This is identical to the observed frequency of the n=3 mode in the burst, as shown in Fig. 4.
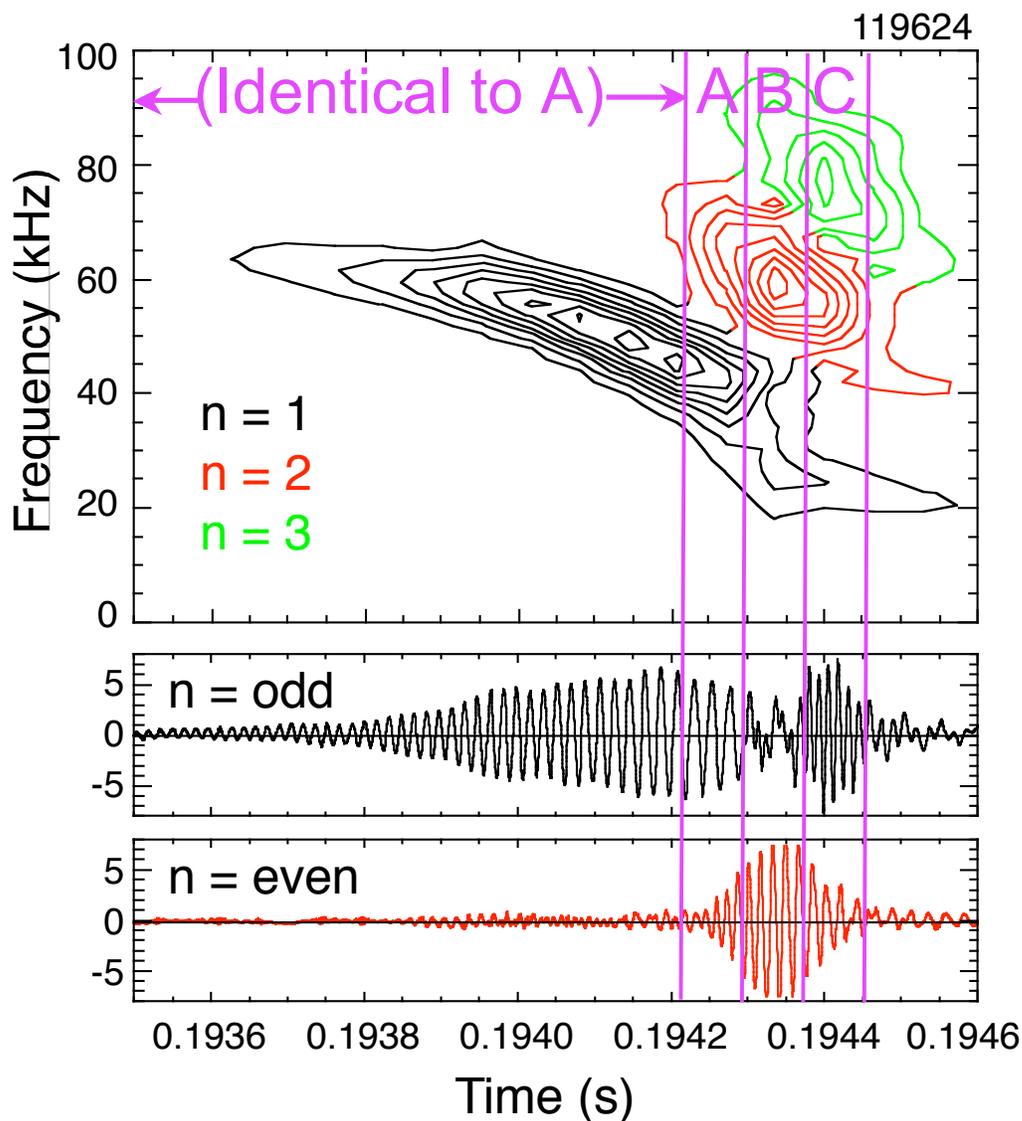
Figure 6: The left panel shows the frequency spectrogram of the burst again, with frame intervals of the fast ion loss probe demarcated by purple vertical lines and labeled by letter. The corresponding fast ion loss distribution images at each time interval are shown in the column at the right, along with the start time of each frame. In the fast ion loss probe images, more parallel-going particles appear at the left side of the frame, and more perpendicular moving particles appear toward the right side of the frame. Particle energy increases going from the lower left to the upper right of each image. A quantitative statement of the pitch angle and gyroradius of the losses is in Figure 8. Note that the camera frames during the interval of frequency sweeping, before frame A, all appear identical in shape, position, and intensity to frame A, meaning that the frequency sweeping n=1 mode does not cause particles to be lost to a position in phase space where they can be detected by the probe. Starting with frame B, there is loss over a broad range of pitch angles, coincident with the temporal overlap of two or more modes.
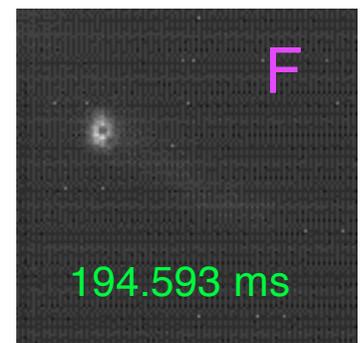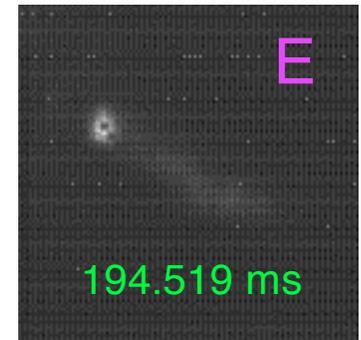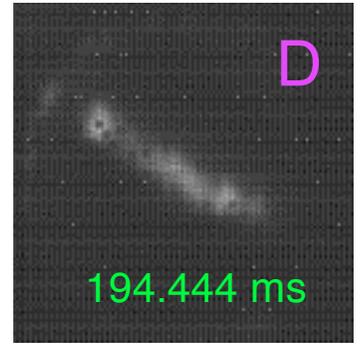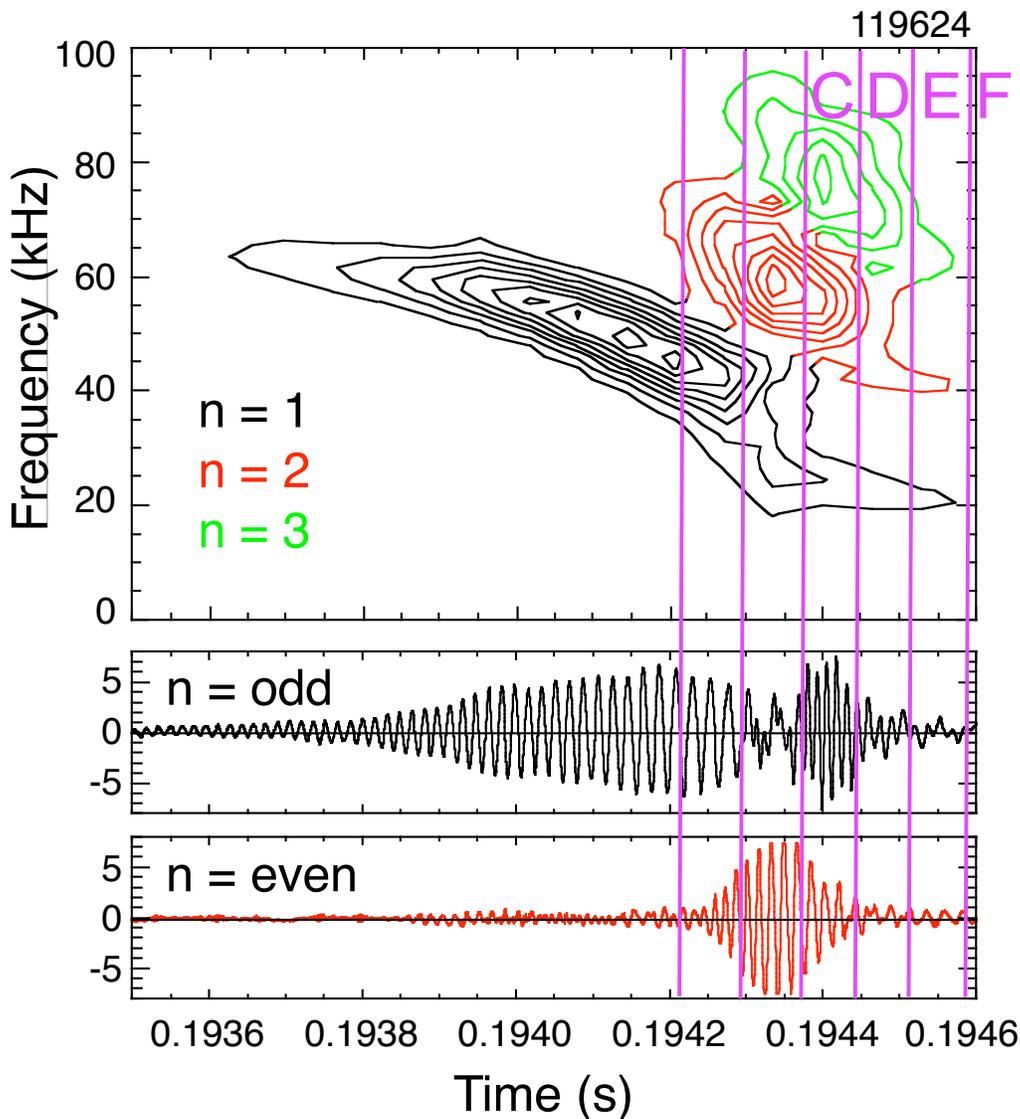
Figure 7: The spectrogram of the burst again, with fast ion loss probe frame intervals later than those in Fig 6 demarcated. The corresponding fast ion loss distribution images at each time interval are shown in the column at the right, along with the start time of each frame In frames D, E, and faintly in F are seen a loss that extends over a wide range of pitch angles, similar to frames B & C in Fig. 6 These also occur during an interval when two different n number modes are present. In frame F, the loss has nearly returned to its pre-burst pitch angle, gyroradius, and intensity.
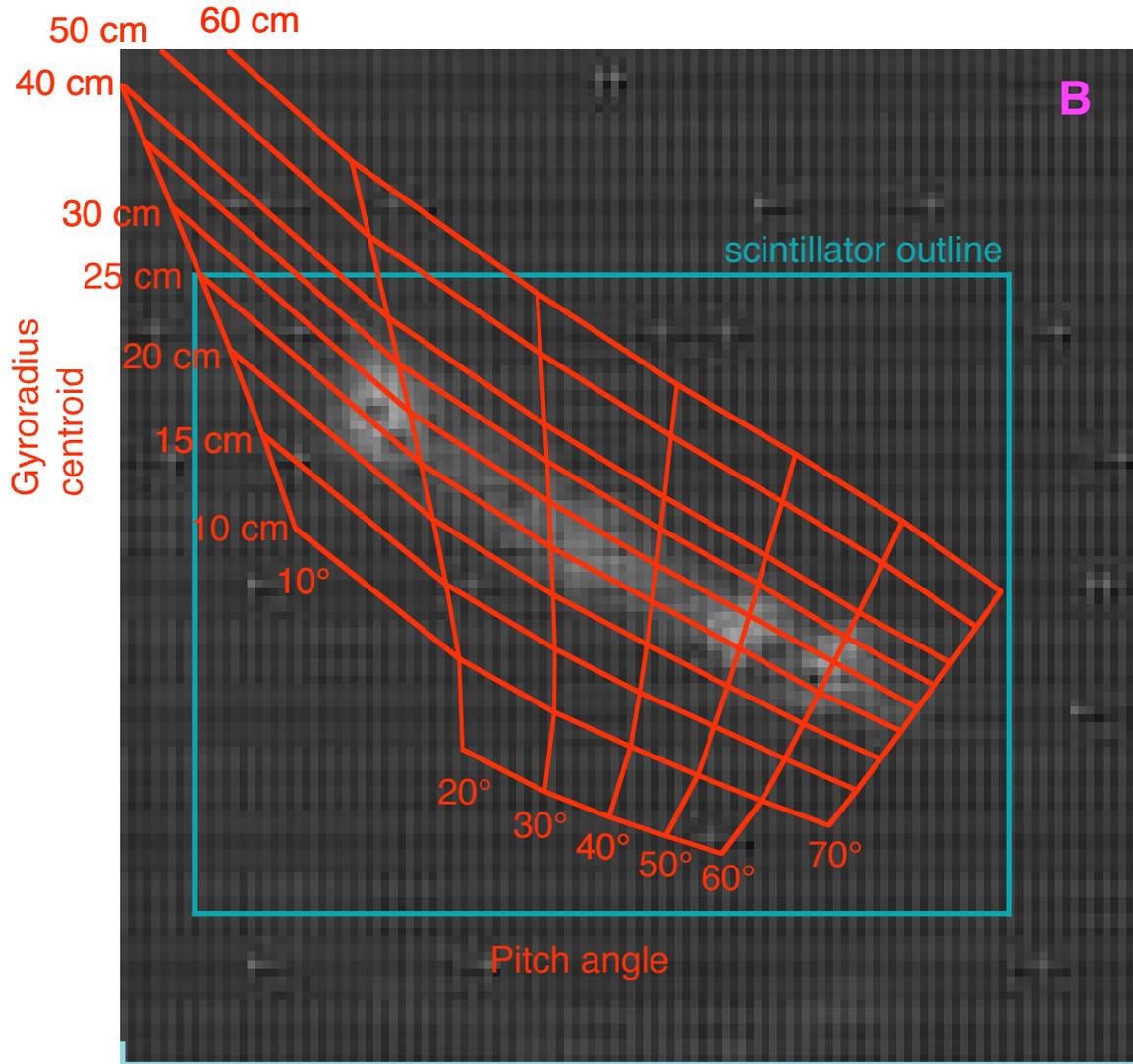
Figure 8: Loss image B from Fig. 6 with superimposed grid of pitch angle and gyroradius centroids. The loss appears at essentially a single gyroradius (25 cm) reasonably commensurate with the gyroradius of 20 cm expected for the 90 keV deuterons being injected. This modest discrepancy between predicted and measured gyroradius is believed to be due to calibration errors in the instrument and not due to any actual acceleration of the particles by the mode. The loss covers a range in pitch angle from 15° to 63°, and the interpretation of the range of pitch angles affected would be altered in only a minor way by the calibration error noted above.